

Effect of Stress Level of Surrounding Soil on Bored Pile Capacity in Sand

Dr. Kais T. Shlash

Building & Construction Department, University of Technology/ Baghdad.

Dr. Mohammed A. Mahmoud

Building & Construction Department, University of Technology/ Baghdad.

Saif I. Akoobi

Building & Construction Department, University of Technology/ Baghdad.

E-Mail: saif.i.akoobi@gmail.com

Received on: 17/9/2012 & Accepted on: 9/5/2013

ABSTRACT

This study deals with assessing the effect of stress level on bearing capacity factor N_q , distribution of shear stresses at soil-pile interface along pile shaft, and presence of critical depth concept for bored piles axially loaded in compression and embedded in dense sand. These investigations are made using finite element method with the employment of a wide range of stresses by using piles with dimensions starting from laboratory dimensions and goes towards field dimensions with embedment ratio L/D range from (15-40). The soil and the interface behavior is modeled using Duncan-Chang hyperbolic soil model with empirical equations account for reduction of angle of internal friction ϕ with increasing in stress level. Bored pile is modeled as a linear elastic material. The results showed a dramatic decrease in bearing capacity factor N_q as length of pile increase. It was also found that the embedment ratio has a significant effect in increasing bearing capacity factor N_q , and the distribution of shear stresses at soil-pile interface is not linear and does not tend to take a constant value beyond a certain depth of pile nor decreases after a certain depth along pile shaft. The fallacy of critical depth also noticed and discussed in this paper.

Keywords: Stress Level, Bored Piles, Finite Element Method, and Hyperbolic Soil Model.

تأثير مستوى أجهاد التربة المحيطة على تحمل ركيزة الحفر في الرمل

الخلاصة

تعنى هذه الدراسة بتقييم تأثير مستوى الأجهاد على معامل سعة التحمل N_q و على توزيع أجهادات القص في منطقة التداخل بين التربة والركيزة و علمبدأ العمق الحرج لركائز حفر محملة تحميلا محوريا ومغموره في تربة رملية قوية. دراسة هذه التأثيرات تم باستخدام طريقة العناصر المحددة عن طريق تمثيل نطاق واسع من الأجهادات بواسطة الأبتداء بركائز بأبعاد مختبرية صغيرة وزيادة الأبعاد الى حد الوصول لركائز بأبعاد موقعية وبنسب غمر مختلفة L/D بين (15-40). تم تمثيل تصرف

التربة ومنطقة التداخل باستخدام نموذج القطع الزائد وتمت إضافة معادلة لهذا النموذج تأخذ بنظر الاعتبار نقصان زاوية الاحتكاك الداخلي θ بزيادة مستوى الأجهاد بينما تم تمثيل تصرف ركيزه الحفر باستخدام النموذج الخطي المرن. أظهرت النتائج نقصلاً شديداً في معامل سعة التحمل N_q بزيادة طول الركيزة وكذلك وجد أن لنسبة الغمر L/D تأثير واضح في زيادة معامل سعة التحمل N_q . لوحظ أيضاً أن توزيع الأجهادات القص في منطقة التداخل بين التربة والركيزة على طول الركيزة لاخطي ولا تميل أجهادات القص الى أن تأخذ قيمة ثابتة او تنقص بعد عمق معين. لوحظ أيضاً وتمت مناقشة عدم وجود أو المغالطة في فرض وجود ما يسمى العمق الحرج.

INTRODUCTION

Prediction of load-carrying capacity of piles in cohesionless soils has been and is still one of the most challenging problems facing geotechnical engineers. The problem is complex and difficult due to the lack of understanding of the phenomena of soil-pile interaction and the limited quantity and inexact quality of subsurface soil information that can be provided for analysis. Due to this, piles behavior was studied using field tests, centrifuge tests, small scale model tests, and numerical techniques.

Laboratory-scale investigations into pile behavior remain popular because of the high cost of field testing and the possibility of achieving specific soil characteristics in a laboratory environment. Model pile tests in sand have been performed in laboratory test chambers for many years (Lehane and White, 2005). Extrapolation of these experimental results to full-scale conditions is hampered, however, by the uncertainty surrounding scale, size effects and stress level effects. These effects should be studied rigorously to overcome the limitation of these experiments. The present study deals with effect of stress level

BACKGROUND

Estimation of static pile capacity of bored piles in compression

A pile subjected to axial load will carry the load partly by shear generated along the shaft and partly by normal stresses generated at the base of pile, so the ultimate load of bored pile subjected to compression load can be estimated using the well-known formula:

$$Q_T = Q_s + Q_b \quad \dots (1)$$

Where, Q_T is the total load the pile can handle, Q_s is the load carried by pile shaft and Q_b is the load carried by pile base.

$$Q_s = 0.5 \cdot P \cdot K_s \cdot \sigma_{vb} \cdot \tan \delta \dots (2)$$

Where, P is the pile perimeter, K_s is the coefficient of lateral earth pressure, σ_{vb} is the vertical stress of soil at level of pile base, and δ is the angle of friction between pile and soil.

$$Q_b = A_b (\sigma_{vb} \cdot N_q) \quad \dots (3)$$

Where, A_b is the area of pile base; and N_q is the bearing capacity factor for deep foundations and is a function of the angle of internal friction. Relations of N_q versus ϕ have been proposed by various authors. Due to the space limitation the description of these relations is not presented in this paper (see Tomlinson and Woodward 2008, Fleming et al. 2008).

Critical depth concept

In equations (2) and (3), as length of pile increase the bearing capacity increase due to the increase in overburden pressure, but for design purposes this increase has a limit value beyond which there is no further increase. The major fact that led to limit the capacity of pile is the critical depth concept. The critical depth is define as the depth below which end-bearing resistance and average shaft resistance in homogenous soil no longer increase in proportional to the effective stress, but become constant. The first who noticed this phenomenon is Kerisel in (1964) from a model tests results. He found that the shaft resistance and end bearing of pile does not necessarily increase linearly with depth but reach a constant value beyond a certain depth, he call it "critical depth". Further support for this concept was made by Vesic (1967) and Meyerhof (1976). Vesic in 1967 noticed that the shaft resistance reach a peak value at a critical depth and then start to decrease until reaching its minimum value at pile tip as shown in Figure (1). Meyerhof in 1976 made a further support for this concept by extensive tests on wide range of piles in different sandy soils. Others donot support this concept and justified the distribution of shear stresses to residual loads effect ((Al-Tae et al., (1992, 1993), Fellenius and Al-Tae, (1995, 1996)).

Residual loads are the loads that appear along sides of pile and beneath pile toe due to installation process (i.e. boring or driving). By using finite element method the presence of critical depth can be checked by investigating the distribution of shear stresses along pile shaft and checking if any limiting value of piles capacities were reached to make further contribution in support of this concept or not which in turn will lead to more understanding of the behavior of deep foundations.

EFFECT OF STRESS LEVEL ON ANGLE OF INTERNAL FRICTION

Variations of maximum achieved friction angle in the standard shear tests with normal or confining pressure had been reported by different researchers (Veiskarami et al., 2011). This variation achieved by changing stress is called 'stress level effect' and considered as one of the major causes of scale effect. The shear strength of the sandy soil is mainly depends on angle of internal friction and this friction angle is highly dependent on stress level. There is a problem arise with question 'did this variation have a great effect on bearing capacity' and 'if it did, what value of friction angle should be used for safe and economical design'. Many researchers studied the variation of friction angle of sand with stress level.

Lee and Seed, (1967) presented data from dense Ottawa sand and dense Sacramento River sand which shows a decrease in friction angle with an increase in confining pressure.

Bolton, (1986) collected data of triaxial and plain strain shear tests for 17 types of sand from different places around the world and by analyzing of these data; he proposed a simple equations for triaxial and plane strain tests correlate the maximum mobilized friction angle with the mean stress level:

$$\phi_{\text{mobilized}} = \phi_{c,v} + 5 I_R \quad (\text{In plane-strain condition}) \quad \dots (4)$$

$$\phi_{\text{mobilized}} = \phi_{\text{c.v}} + 3 I_R \quad (\text{in triaxial condition}) \quad \dots (5)$$

$$I_R = R_D(Q - \ln(\sigma)) - R \quad 0 \leq I_R \leq 4 \quad \dots (6)$$

Where, $\phi_{\text{c.v}}$ angle of internal friction at constant volume, R_D relative density of sand, Q & R constants and will be discussed below, and σ the mean effective stress.

Bolton proposed that the constants in the above two equations (Q & R) can be taken equal to 10 and 1 respectively, while Salgado et al., (2000) performed a series of laboratory tests on Ottawa sand with fines content range from (0-20%) by weight and provide equation in the same form of Bolton's equations but the values of constants (Q & R) differ from Bolton's constants and for a wide range of fine content. Summary of these constants as proposed by Salgado et al. is shown in Table (1).

Kumar et al., (2007) performed a number of direct shear tests on Bangalore sand to check the validity of Bolton's and Salgado et al.'s equations. They proposed a little modification on the equation to be in the form:

$$\phi_{\text{mobilized}} = \phi_{\text{c.v}} + 3.5 I_R \quad \dots (7)$$

EFFECT OF STRESS LEVEL ON BEARING CAPACITY OF SOIL

Several researchers have observed and reported that the bearing capacity of shallow foundations does not increase without bound and N_y (third term in well-known bearing capacity equation) decreases when the foundation size increases (De Beer, 1963; Clark, 1998; Kumar & Khatri, 2008; Yamamoto et al., 2009; Veiskarami et al., 2011). The reduction of N_y comes from the decrease of the mobilized angle of internal friction as foundation size increases (i.e. stress level increase). This effect is not rigorously studied for deep foundation in spite of the higher stresses expected to appear in case of deep foundations due to overburden pressure and the stresses transferred from the structures to soil by deep foundations. Only few works of such effect are available in literature (e.g. Craig and Sabagh, 1994 and Kuwajima et al., 2009). Also, this effect will make a doubt about the validity of small-scale models in simulation of real filed problem and the validity of equation and charts from such experiments to apply in filed problems. However, a study like this needs an extensive program of field tests or centrifuge modeling, which are not readily available due to the high cost of such program. With the presence of finite element method such a program can acceptably be established with relatively low cost and it only requires a finite element program and a computer.

OBJECTIVES OF THE STUDY

The main objectives of this study include the following points:

1. Investigating the effect of embedment ratio (L/D) and stress level on bearing capacity factor N_q for bored piles embedded in dense sand.
2. Studying the effect of stress level on distribution of shear stresses along pile-soil interface.
3. Checking the validity of critical depth concept for bored piles.

To achieve the objectives above, an attempt to pass through a wide range of stress levels starting from laboratory stresses (i.e. 1-g model) towards field stresses

was made in this study. Five embedment ratios (L/D) used in this study which were (15, 20, 25, 30 and 40). The lengths and diameters of piles used are shown in Table (2).

FINITE ELEMENT PROGRAM USED

Description of the Program

The finite element computer program modified by Al-Shlash (1979) in FORTRAN language was used in the finite element analysis carried out during this research. Four different types of element can be used in the finite element mesh in solving, soil, structural, and soil structure interaction problems under plane or axisymmetrical conditions. Three models can be used in this program to represent the behavior of the soil and the soil structure interaction, these models are, linear elastic model, (ii) bilinear elastic completely plastic model, (iii) hyperbolic incremental stress dependent.

Two models used in this work which are the hyperbolic, incremental, stress dependent, nonlinear technique (Duncan and Chang, 1970) on primary loading with a different stress dependent modulus on unloading or reloading to simulate soil behavior and linear elastic model to simulate concrete bored pile behavior.

Development of the Program

Before using this program, simple development was made on the hyperbolic soil model by inserting Bolton's empirical equation (5) to input the effect of stress level in reducing the angle of internal friction for sandy soil as discussed earlier. By providing the program with critical state friction angle ϕ_{cs} and the relative density, the program will calculate the angle of internal friction for each element before calculating tangent modulus (E_t) and hence, the effect of stress level will be incorporated in hyperbolic soil model. The assumption of critical state friction angle independent on stress level was made in this development. Few Reports indicated that the critical state friction angle might depend on stress level (Sabagh,1983; Chu, 1995 & Clark, 1998), but this required further investigation as there are more evidences in literature that critical state friction angle is independent of stress level (e.g. Bolton, 1986; Salgado et al., 2000; Salgado, 2006; Kumar et al., 2007; Chakraborty & Salgado, 2010).

Verification of the Program

To test the capability of the developed program to estimate bearing capacity of pile, a problem selected from literature and reanalyzed using this program. The selected problem involves a (10 cm) model pile with a length of (≈ 160 cm). This pile was tested by Vesic (1975) in medium dense Chattahoochee River sand and reanalyzed by using finite element method by (Armaleh & Desai, 1987), from whom the non-linear hyperbolic soil properties are adopted and shown in Table (3). It should be mentioned that the material properties available in reference not contain a critical state friction angle, for this reason this parameter is estimated by inverse Bolton's equation by knowing triaxial angle of internal friction and relative density of soil. In this problem the pile is treated as a linear elastic material and its properties are shown in Table (2). The finite element mesh for this problem is shown in Figure (2). Five points isoparametric elements are used in forming finite element mesh to model the axi-symmetric soil-pile problem. The load settlement curve obtained from the present analysis and the load settlement curve obtained by Vesic are presented in Figure (3) for comparison purpose. It is seen that, the load displacement curve using

this program with the developed hyperbolic soil model shows a good agreement with the results from Vesic test.

PROBLEMS GEOMETRY

All problems involved bored piles embedded in dry dense sandy soil with various diameters and lengths. The pile-soil system is treated as an axi-symmetric problem in two dimensional finite element analyses. Due to the symmetry of loading and geometry, only one radian of the pile-soil system is considered. Boundary of the soil in FEM depends on the diameters and the lengths of bored piles.

The effect of soil mass on pile response diminishes when the width is greater than $(20D)$ and the height of soil mass is $(L + 20D)$, in which, L is the length of pile and D is the diameter of pile (Chik et al., 2009). So the boundaries are taken as $(20D)$ for width and $(L + 20D)$ for height of the soil. In order to use same mesh dimensions in different embedment ratios, the height of the mesh for all (L/D) ratios are taken on the basis of greater embedment ratio (i.e. $(L/D) = 40$). Five points isoparametric elements are used in forming finite element mesh to model the axi-symmetric soil-pile problem. The nodal points along the centerline and those on the far right vertical boundary are assumed to move only in vertical direction, while the nodal points in the bottom of the boundary are assumed to be fixed in vertical and horizontal directions. The finite element mesh for piles with embedment ratio $(L/D)=40$ is shown in Figure (4). In this figure the mesh dimensions explained in term of lengths and diameters of piles. Piles with other embedment ratios have same mesh dimensions shown in Figure (4); only the length of piles will be less than that of pile in Figure (4).

MATERIALS PROPERTIES

In this paper the dense sand was used to study the effect of stress level. The soil is modeled using non-linear hyperbolic soil model while, bored pile is assumed to be linear elastic material. The nonlinear hyperbolic properties of dense sand and nonlinear soil –pile interface were adopted from Haddad (1997) and shown in Table (4) and Table (5) respectively. It should be noted that the available data in literature from which the hyperbolic parameters were taken does not contain critical state friction angle of sand, for this causation this parameter was obtained by back calculating of Bolton's empirical equation (equation (5)) by knowing maximum mobilized fraction angle and the relative density of sand. The linear elastic properties of the concrete bored pile are shown in Table (3).

RESULTS

Load – Settlement Relations

The load - settlement curves obtained by finite element program for bored piles explained in Table (2) are shown in Figures (5) to (11) for piles with embedment ratio $(L/D) = 15$ embedded in dense sand. All the embedment ratios gave the same trend shape of load-settlement relations, so, these results are not shown here due to the lack of space.

These Figures indicate that the load - settlement relation approximately have the same trend shape for all diameters and lengths. When the loading process on the pile is starting, the pile settlement response seems to be very close to linear relation due to small settlement value. After this stage and with continuing the loading process, the

non-linearity behavior of soil is appeared and providing a visible curvature as soil elements start to fail causing a significant increase in rate of settlement and provide a hyperbolic shape for load - settlement relation. In the final stage of loading, all elements around the pile will be failed and causing a displacement overshoots due to rapid reduction in the tangent modulus.

It can be seen from load - settlement curves that the punching type failure controls for all stress ranges and as embedment depth increases the capacity of piles increase for all range of stresses. This observation gives first indication about the fallacy of critical depth.

Ultimate Load, Ultimate Shaft Resistance, and Ultimate End Bearing

In this study, the failure criteria proposed by Terzaghi (10% D) was used to predict the ultimate load that the pile can handle as shown in Figure (5). The end bearing and shaft resistance are computed as follow:

1. The shaft resistance Q_s is computed by integrating the tangential shear τ in the interface elements. Thus:

$$Q_s = \sum_{i=1}^{tot} \tau_i \Delta L_i D_i \pi \quad \dots (8)$$

Where, τ_i shear stress in interface element, ΔL_i length of interface element, D_i diameter of pile, and tot total number of interface elements.

2. The finite element program used in this study calculates the stress at the centroid of the elements not in the edges of elements, due to this the end bearing resistance of pile Q_b is computed from equilibrium consideration by subtracting the shaft resistance obtained in step 1 from the total ultimate load from load - settlement curve. Thus:

$$Q_b = Q_T - Q_s \quad \dots (9)$$

A summary of ultimate load, ultimate shaft, and end bearing resistance for all piles in dense sand are shown in Table (6).

Effect of Stress Level on Bearing Capacity Factor N_q

The bearing capacity factor N_q is the most important parameter in estimating the end bearing capacity for piles in sand in the absence of field tests such as (SPT) and (CPT). In this section, the effect of stress level in combination with embedment ratio (L/D) on bearing capacity factor N_q will be discussed. The bearing capacity factor N_q is obtained from the ultimate end bearing capacity for each pile by back calculation, thus N_q will be:

$$N_q = \frac{\text{Ultimate end bearing}}{\frac{\pi}{4} D^2 \gamma L} \quad \dots (10)$$

To assess the effect of stress level on bearing capacity factor N_q , the values of the bearing capacity factor N_q computed from equation (10) are plotted against the lengths of piles embedded in dense sand in Figure (12). The mobilized angles of internal friction based on Bolton's equation at ultimate load (10% D) in the centroid of the element below pile tip for all lengths of piles embedded in dense sand are

plotted in Figure (13). Figure (12) indicates that bearing capacity factor N_q is dramatically decreases as length of piles increase (i.e. stress level increase). This reduction is attributed to the reduction in angle of internal friction with increasing stress level Figure (13) and it is well known that N_q is a function of angle of internal friction, so, N_q is a function of stress level also. These results are in agreement with the observations of (Craig and Sabagh, 1994; Kuwajima et al., 2009), whom noticed also same trend in reduction of bearing capacity factor as stress level increases. It can be seen that the rate of decrease in N_q value is decreasing as length of piles increase until it reaches a constant value beyond a certain depth which is approximately equal to (18 m). Beyond this depth the value of bearing capacity factor N_q will be independent of stress level. This independency came from the following reasons:

- 1- Logarithmic relation between mobilized angle of internal friction and stress level.
- 2- The tendency of mobilized angle of internal friction to become almost constant or much less sensitive to increasing in applied stress on soil element in high stress range where its value approaches to the critical state friction angle and as angle of internal friction becomes constant, the bearing capacity factor N_q also tend to become constant.
- 3- The less sensitivity of bearing capacity factor to change in mobilized angle of internal friction as its value starts to approach critical state friction angle.

From these observations, it can be concluded that extrapolating results for bearing capacity factor N_q from small scale 1-g model test to field scale can produce extreme error and overestimate the end bearing pile capacity.

Meyerhof (1983) assumed that for long piles the mobilized angle of internal friction in ultimate state at pile tip is close to the value of the critical state friction angle. Based on the analyses from this study and from Figure (13), it can be concluded that this assumption is not valid for dense sand because the mobilized friction angle is higher by five degrees than critical state friction angle for the same pile. It can be seen also from Figure (12) that, as embedment ratio (L/D) increases the bearing capacity factor increases until (18 m) depth beyond this depth, the embedment ratio (L/D) effect will approximately vanishes and all embedment ratios will give the same value for the bearing capacity factor N_q . The tendency of decrease of bearing capacity factor N_q with increasing length can explain why the rate of increase in ultimate pile capacity decreases as pile length increase. This observation overrides the theory of the past which attributed the rate of decreasing in pile capacity as length of pile increase to the critical depth theory. It should be mentioned that the value of N_q computed within this study is derived by assuming tangent modulus of elasticity after failure equal 10% of tangent modulus of elasticity before failure, so the values obtained from this study can be considered as a lower bound values. Much higher values can be obtained if higher value for modulus of elasticity after failure is assumed for failed elements in the finite element analysis.

Effect of Stress Level on Distribution of Shear Stresses Generated at the Interface along the Pile Shaft

By investigating profiles of shear stress generated at pile shaft in ultimate state (10% D) for all embedment ratios in dense sand, it is clear that all profiles have same trend. Due to this only the profiles for shear stresses generated at piles shaft for embedment ratio ($L/D = 25$) are presented in Figures (14) to (20) and will be discussed below:

From these Figures, the followings remarks can be put forward:

- 1- There is no pronounced effect of stress level on the distribution of shear stresses generated along pile shaft.
- 2- The distribution of shear does not reach a constant value beyond which no further increase nor decreases after a certain depth which equal to half of pile length as explained by Vesic (1967) as shown in Figure (1).
- 3- This distribution of shear stresses along pile shaft does not linearly increase as assumed in conventional static design equations by many authors.

It can be seen that the distribution of shear along piles shafts is random and it tends to increase as length of pile increase (i.e. increase in overburden pressure). This finding agrees with the finding of (Gurtowski & Wu, 1984; Mey et al., 1985; and Yen et al., 1989), whom also noticed same random distribution of shear stresses along piles shafts from instrumented piles during piles load tests at field. The random and non-linear shapes of shear along piles shafts may be attributed to the dependency of developed shear stress on the radial effective stress and the changes in the radial effective stress during loading stages due to rotation of principle stress as explained by Lehane et al., 1993 and Jardine et al., 1998.

Critical Depth Concept

The critical depth concept is still adopted in recent foundations text books (e.g. Reese et al., 2006; Tomlinson and Woodward, 2008; Rajapakse, 2009) but, numerical analysis carried out during the present study makes further contribution in support of doubts about the critical depth concept by the following evidences:

1. No limiting value was noticed for pile capacity for all stress ranges with all investigated embedment ratios as shown in Table (5) and presented in figure (21) for pile diameter 60 cm as an example.
2. A reduction in the angle of internal friction with stress level increase (i.e. length increase) and the dependency of bearing capacity factor N_q on it as discussed earlier in section (10.3) and shown in Figures (12) and (13) may leads to error and misleading in interpretation of results from load cells or strain gauges attached to instrumented piles, and lead to believe in critical depth concept.
3. The distribution of shear stresses does not reach a constant value beyond which no further increase nor decrease occur at a certain depth for all stress ranges. The profiles of shear stresses generated at soil-pile interface show the tendency to increase with random fashion and does not reach a constant value as discussed earlier in section (10.4) and shown in Figures (14) to (20).

CONCLUSIONS

From the present numerical analyses of bored piles embedded in sandy soil for wide range of stress levels, the following conclusions can be made:

1. The extrapolating of results from small scale 1-g model or using a small scale 1-g model to study the behavior of piles embedded in medium or dense sand are not accurate if the stress level effect is neglected. The stress level effect should be incorporated and taken with care in such stress level dependent soils.
2. The bearing capacity factor N_q decreases dramatically as length of pile increases until it reaches approximately a constant value beyond (18 m) depth for pile embedded in dense sand, due to the effect of stress level in reducing the mobilized angle of internal friction and the logarithmic relation between mean stress and the mobilized angle of internal friction.
3. The bearing capacity factor N_q increases as embedment ratio L/D increases until (18 m) depth for piles embedded in dense sand beyond which, there is no effect for embedment ratio on bearing capacity factor N_q .
4. The distribution of shear stresses in soil-pile interface along pile shaft is random, non-linear, and it tends to increase with increasing overburden pressure.
5. For all piles considered in this study, the effect of critical depth is not appeared.

REFERENCES

- [1].Al-Shlash, K.T. (1979), "Application of the Finite Element Method in Assessing the Behavior of Tie-Back Walls", Ph.D. Thesis, University of Sheffield, England.
- [2].Al-Taee, A., Evgin, E., and Fellenius, B.H. (1992), "Axial Load Transfer for Piles in Sand. II. Numerical Analysis", Canadian Geotechnical Journal, Vol. 29, pp. 21-30.
- [3].Al-Taee, A., Evgin, E., and Fellenius, B.H. (1993), "Load Transfer for Piles in Sand and the Critical Depth", Canadian Geotechnical Journal, Vol. 30, pp. 455-463.
- [4].Armaleh, S., and Desai, C.S. (1987), "Load Deformation Response of Axially Loaded Piles", Journal of Geotechnical Engineering, Vol. 113, No. 12, pp. 1483-1500.
- [5].Bolton, M.D (1986), "The Strength and Dilatancy of Sands", Géotechnique, Vol. 36, No. 1, pp. 65-78.
- [6].Chakraborty, T., and Salgado, R., (2010), "Dilatancy and Shear Strength of Sand at Low Confining Pressures", Journal of Geotechnical and Geoenvironmental Engineering, Vol. 136, No. 3, pp. 527-532.
- [7].Chik, Z.H., Abbas, J.M., Taha, M.R, and Shafiqu, Q.S.M. (2009), "Lateral Behavior of Single Pile in Cohesionless Soil Subjected to both Vertical and Horizontal Loads", European Journal of Scientific Research, Vol. 29, No. 2, pp. 194-205.
- [8].Chu, J. (1995), "An Experimental Examination of the Critical State and Other Similar Concepts for Granular Soils", Canadian Geotechnical Journal, Vol. 32, pp. 1065-1075.
- [9].Clark, J.I. (1998), "The Settlement and Bearing Capacity of Very Large Foundations on Strong Soils: 1996 R.M Hardy Keynote Address", Canadian Geotechnical Journal, Vol. 35, pp. 131-145.
- [10].Craig, W.H., and Sabagh, S.K (1994), "Stress-Level Effects in Model Tests on Piles", Canadian Geotechnical Journal, Vol. 31, pp. 28-41.

- [11].De Beer, E. E. (1963), "The Scale Effect in Transposition of the Results of Deep Sounding Tests on the Ultimate Bearing Capacity of Piles and Caisson Foundations", *Geotechnique*, Vol. 13, No.1, pp. 39–75 (as cited by (Yamamoto et. al., 2009)).
- [12].Duncan, J. M. and Chang (1970), "Nonlinear Analysis of Stress and Strain in Soils", *Journal of Soil Mechanic and Foundation Engineering Division*, Vol. 96, No. SM5, pp. 1929-1953.
- [13].Fellenius, B.H., and Altaee, A.A. (1995), "Critical Depth: How it Came into Being and Why it Does Not Exist", *Proceeding of International Conference in Civil Engineering, Geotechnical Engineering Section*, April, 1995, Vol. 113, pp. 107-111.
- [14].Fellenius, B.H., and Altaee, A.A. (1996), "Discussion: Critical Depth: How it Came Into Being and Why it Does Not Exist", *Proceeding of International Conference in Civil Engineering, Geotechnical Engineering Section*, October, 1996, Vol.119, pp. 244-245.
- [15].Fish, J., and Belytschko, T. (2007), "A First Course in Finite Elements", John Wiley & Sons Ltd, West Sussex.
- [16].Fleming, K., Weltman, A., Randolph, M., and Elson, K. (2008), "Piling Engineering", 3rd Edition, Taylor & Francis, London and New York.
- [17].Gurtowski, T. M., and Wu, M. J. (1984), "Compression Load Test on Concrete Piles in Aluminium", In *Symposium of Analysis and Design of Pile Foundation*, pp. 138-153. New York: American Society of Civil Engineers.
- [18].Haddad, O.F. (1997), "Effect of Bentonite on the Friction between Soil and the Materials Used in Deep Foundations Construction by F.E.M", M.Sc. Thesis, University of Technology, Iraq.
- [19].Jardine, R.J., Overy, R.F., and Chow, F.C. (1998), "Axial Capacity of Offshore Piles in Dense North Sea Sands", *Journal of Geotechnical and Geoenvironmental Engineering*, Vol. 124, No. 2, pp. 171-178.
- [20].Kerisel, J. (1964), "Deep Foundations-Basic Experimental Facts", *Proceeding of International Conference on Deep Foundations*, Mexico City (as cited by (Fellenius & Altaee, 1995)).
- [21].Kumar, J., and Khatri, V.N. (2008), "Effect of Footing Width on Bearing Capacity Factor N_f for Smooth Strip Footings", *Journal of Geotechnical and Geoenvironmental Engineering*, Vol. 134, No. 9, pp. 1299-1310.
- [22].Kumar, J., Raju, K.V.S.B., and Kumar, A. (2007), "Relationships between Rate of Dilation, Peak and Critical State Friction Angles", *Indian Geotechnical Journal*, Vol. 37, No. 1, pp. 53–63.
- [23].Kuwajima, K., Hyodo, M., and Hyde, A. (2009), "Pile Bearing Capacity Factors and Soil Crushability", *Journal of Geotechnical and Geoenvironmental Engineering*, Vol.135, No. 7, pp. 901-919.
- [24].Lee, K. L. and Seed, H. B. (1967), "Drained Strength Characteristics of Sands" *Journal of the Soil Mechanics and Foundations Division*, Vol. 93, No. SM6, pp. 117-141.
- [25].Lehane, B. M., and White, D. J. (2005), "Lateral Stress Changes and Shaft Friction for Model Displacement Piles in Sand" *Canadian Geotechnical Journal*, Vol. 42, pp. 1039-1042.
- [26].Lehane, B.M., Jardine, R.J., Bond, A.J., and Frank, R. (1993), "Mechanism of Shaft Friction in Sand from Instrumented Pile Tests", *Journal of Geotechnical Engineering*, Vol. 119, No. 1, pp. 19-35.

[27].Mey, R., Oteo, C. S., Sanchez Del Rio, J., and Seriano, A. (1985), “ Field testing on Large Driven Piles”, Proc. 11th International Conference in Soil Mechanics, San Francisco 3, pp. 1559-1564 (as cited by (Randolph et. al., 1994)).

[28].Meyerhof, G.G. (1976), “Bearing Capacity and Settlement of Pile Foundations”, Journal of Geotechnical Engineering, Vol. 102, No. GT3, pp. 195-228.

[29].Meyerhof, G.G. (1983), “Scale Effects of Ultimate Pile Capacity”, Journal of Geotechnical Engineering, Vol. 109, No. 6, pp. 797-806.

[30].Rajapakse, R. (2008), “Pile Design for Structural and Geotechnical Engineers”, Butterworth-Heinemann, New York.

[31].Reese, L.C., Isenhower, W.M., and Wang, S. (2006), “Analysis and Design of Shallow and Deep Foundations”, John Wiley & Sons, Inc., Hoboken, New Jersey.

[32].Sabagh, S.K. (1983), “Model Pile Tests in Sand Using the Centrifuge”, Ph.D. Thesis, University of Manchester, United Kingdom.

[33].Salgado, R. (2006), “The Engineering of Foundations”, 1st Edition, McGraw-Hill book company, New York.

[34].Salgado, R., Bandini, P., and Karim, A. (2000), “Shear Strength and Stiffness of Silty Sand”, Journal of Geotechnical and Geoenvironmental Engineering, Vol. 126, No. 5, pp. 451-462.

[35].Tomlinson, M., and Woodward, J. (2008), “Pile Design and Construction Practice”, 5th Edition, Taylor & Francis, London and New York.

[36].Veiskarami, M., Jahanandish, M., and Ghahramani, A. (2011), “Prediction of the Bearing Capacity and Load–Displacement Behavior of Shallow Foundations by the Stress-Level-Based ZEL Method”, ScientiaIranica, Vol. 18, No. 1, pp. 16-27.

[37].Vesic, A. S. (1975), “Principle of Pile Foundation Design”, Soil Mechanics Series, 38, Duke University, Durham, N.C (as cited by (Armaleh & Desai, 1987)).

[38].Vesic, A.S. (1967), “A Study of Bearing Capacity of Deep Foundations”, Final Report, Project B-189, Georgia Institute of Technology, Atlanta, GA, Mar

[39].Wehnert, M., and Vermeer, P.A. (2004), “Numerical Analyses of Load Tests on Bored Piles”, Proceeding of the 9th International Conference on Numerical Methods in Geomechanics, Ottawa, Canada, August 25-27, 2004, Vol.1, pp. 1-6.

[40].Yamamoto, N., Randolph, M.F., and Einav, I. (2009), “Numerical Study of the Effect of Foundation Size for a Wide Range of Sands”, Journal of Geotechnical and Geoenvironmental Engineering, Vol. 135, No. 1, pp. 37-45.

[41].Yen, T.L., Lin, H., and Chin, C.T. (1989), “Interpretation of Instrumented Driven Steel Pipe Piles”, Foundation Engineering: Current Principles and Practices, Vol. 2, pp. 1293-1309, New York, American Society of Civil Engineers.

Table (1) the constants Q&R as proposed by Salgado et al., (2000).

Silt (%)	Q	R
0	9.0	0.49
5	9.0	-0.5
10	8.3	-0.69
15 (RD > 38%)	11.4	1.29
15 (RD < 38%)	7.9	0.04
20 (RD > 59%)	10.1	0.85
20 (RD < 59%)	7.3	0.08

Table (2) Bored piles dimensions used in the F.E. analysis.

Diameter (cm)	L/D =15	L/D =20	L/D =25	L/D =30	L/D =40
	Length (m)	Length (m)	Length (m)	Length (m)	Length (m)
2	0.3	0.4	0.5	0.6	0.8
4	0.6	0.8	1	1.2	1.6
8	1.2	1.6	2	2.4	3.2
16	2.4	3.2	4	4.8	6.4
30	4.5	6	7.5	9	12
60	9	12	15	18	-----
120	18	24	30	-----	-----

Table (3) Nonlinear hyperbolic properties of medium sand and linear elastic properties of piles (after Armaleh & Desai, 1987).

Parameters	Soil	Pile
Unit weight γ (kN/m ³)	15	24
Coefficient of at rest earth pressure, k_0	0.463	----
Cohesion intercept c (kPa)	0	----
Max.Angle of internal friction ϕ	35.5	----
Poisson's ratio ν	0.3	0.2
Modulus of elasticity	Variable	2500000
K	909	----
n	0.49	----
R_f	0.89	----
$\phi_{c,s}$	23.5	----
RD (%)	60	----

Table (4) Non-linear hyperbolic properties of dense sand. (after Haddad, 1997).

Parameters	Soil	Pile
Unit weight γ (kN/m ³)	15.6	24
Coefficient of at rest earth pressure, k_0	0.4	----
Cohesion intercept c (kPa)	0	----
Max.Angle of internal friction ϕ	37	----
Poisson's ratio ν	0.3	0.2
Modulus of elasticity	Variable	2500000
K	950	----
n	0.45	----
R_f	0.8	----
E_f (kPa)	0.1 of prefailure ratio	----
ϕ_{c-s}	25	----
$R D$ (%)	70	----

Table (5) Non-linear interface parameters for dense sand –pile interface (after Hadda, 1997).

Material	δ	K_j	n	R_f
Soil-pile interface	33.5	23300	0.27	0.9

Table (6) Summary of ultimate load, ultimate end bearing and ultimate shaft resistance for piles embedded in dense sand.

D (cm)	L (m)	L/D	Ultimate load (kN)	Ultimate end bearing (kN)	Ultimate shaft resistance (kN)
2.0	0.3	15	0.0938	0.0827	0.0111
4.0	0.6	15	0.654	0.571	0.083
8.0	1.2	15	3.675	2.92	0.755
16.0	2.4	15	22.514	16.875	5.639
30.0	4.5	15	131.503	93.083	38.42
60.0	9	15	872.48	515.27	357.21
120.0	18	15	5782.0	3200.24	2581.76
2.0	0.4	20	0.128	0.109	0.019
4.0	0.8	20	0.808	0.627	0.181
8.0	1.6	20	5.605	4.5	1.105
16.0	3.2	20	35.923	24.64	11.283
30.0	6	20	212.305	141.63	70.675
60.0	12	20	1240.59	689.73	550.86
120.0	24	20	9138.13	4045.216	5092.914
2.0	0.5	25	0.1614	0.14	0.0214
4.0	1	25	1.051	0.8	0.251
8.0	2	25	7.787	5.52	2.267

16.0	4	25	51.32	32.74	18.58
30.0	7.5	25	280.01	169.48	110.53
60.0	15	25	1865.32	663.89	1201.43
120.0	30	25	12472.58	4705.65	7766.93
2.0	0.6	30	0.213	0.173	0.04
4.0	1.2	30	1.567	1.207	0.36
8.0	2.4	30	10.84	7.87	2.97
16.0	4.8	30	63.55	37.21	26.34
30.0	9	30	370.329	199.31	171.019
60.0	18	30	2370.39	871.43	1498.96
2.0	0.8	40	0.328	0.254	0.074
4.0	1.6	40	2.5	1.8	0.7
8.0	3.2	40	17.33	11.81	5.52
16.0	6.4	40	102.85	57.283	45.567
30.0	12	40	601.78	249.13	352.65

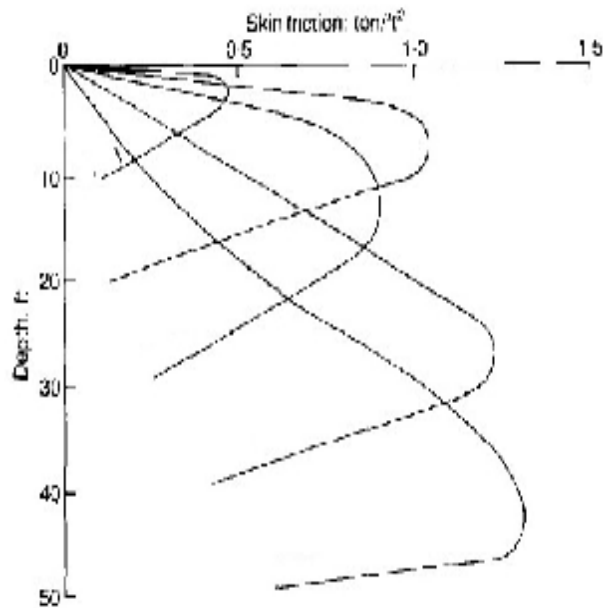


Figure (1) Distribution of shaft friction along pile shaft (after Vesic, 1967).

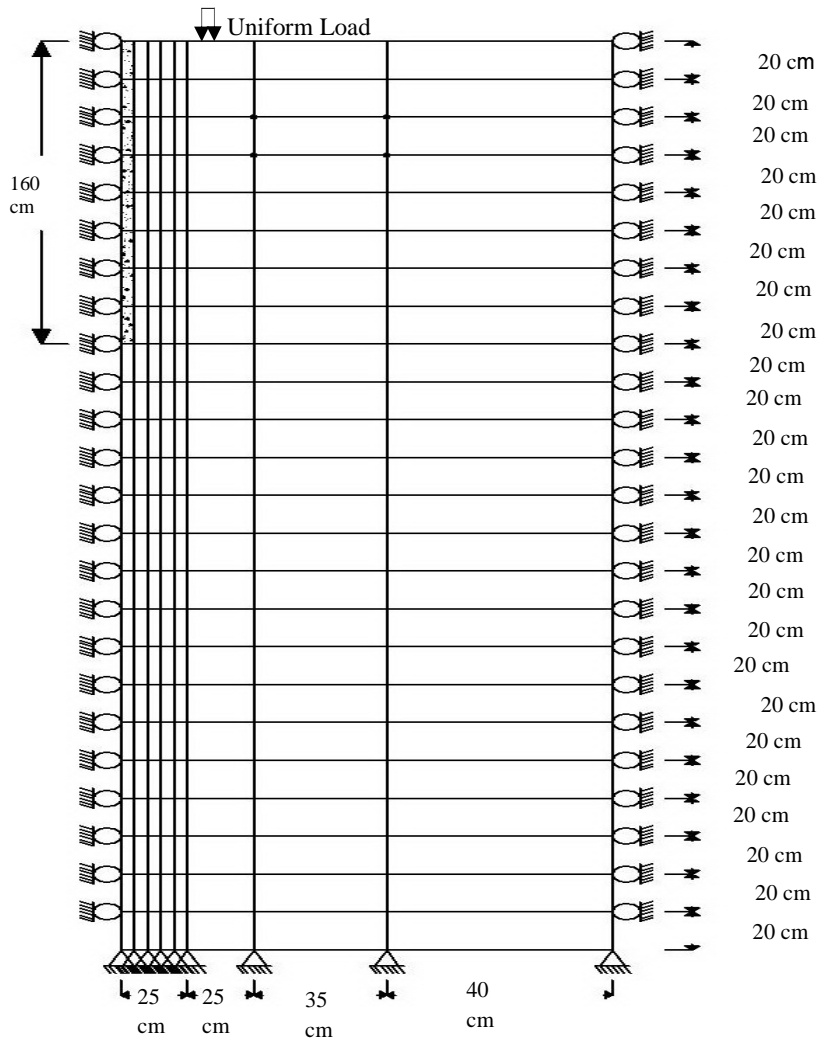


Figure (2) The finite element mesh for verification problem.

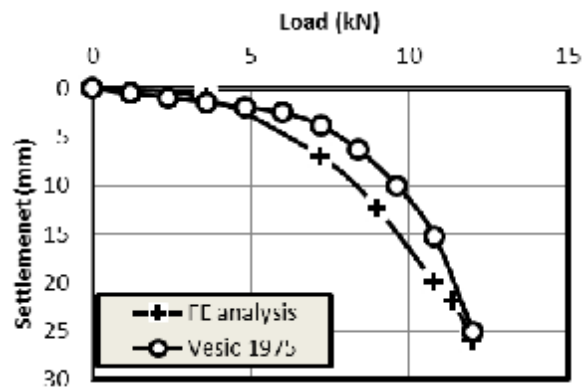


Figure (3) Comparison between Vesic (1975) and the present program results of load-settlement curve for the pile test.

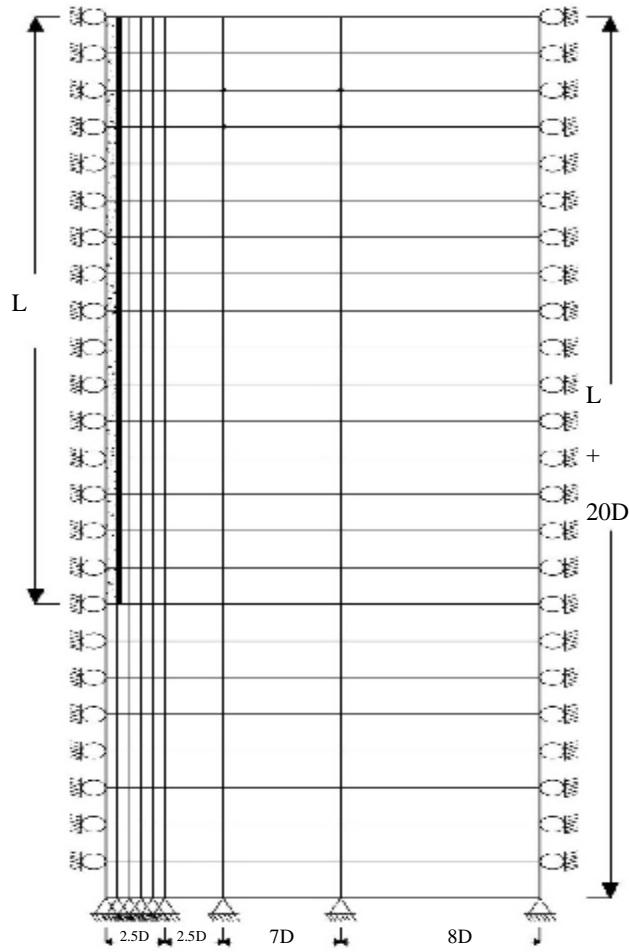


Figure (4) The finite element mesh for piles with $(L/D) = 40$.

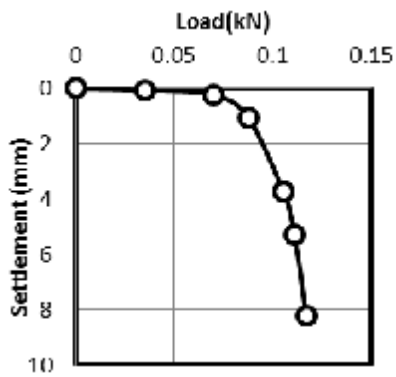


Figure (5) Load-Settlement relation of pile with $D=2$ cm and $L=30$ cm.

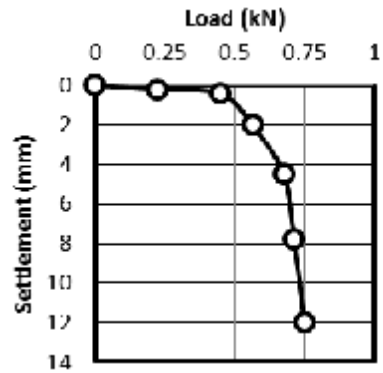


Figure (6) Load-Settlement relation of pile with $D=4$ cm and $L=60$ cm.

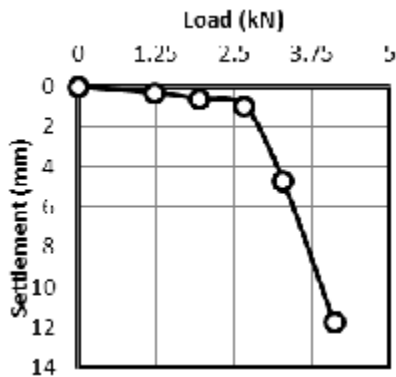


Figure (7) Load-Settlement relation of pile with D= 8 cm and L= 120 cm.

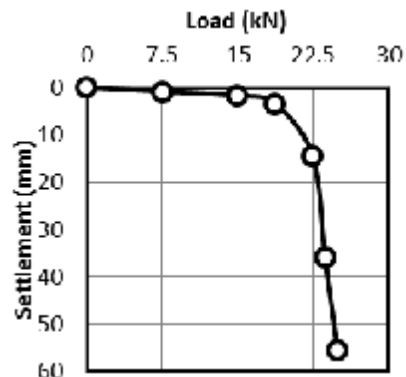


Figure (8) Load-Settlement relation of pile with D= 16 cm and L= 240 cm.



Figure (9) Load-Settlement relation of pile with D= 30 cm and L= 450 cm.

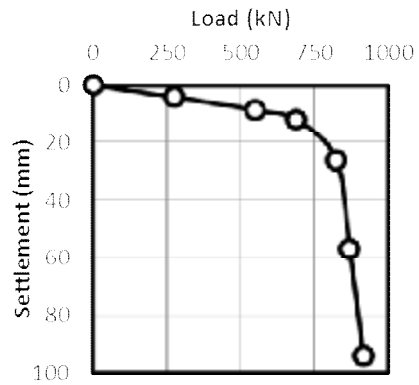


Figure (10) Load-Settlement relation of pile with D= 60 cm and L= 900 cm.

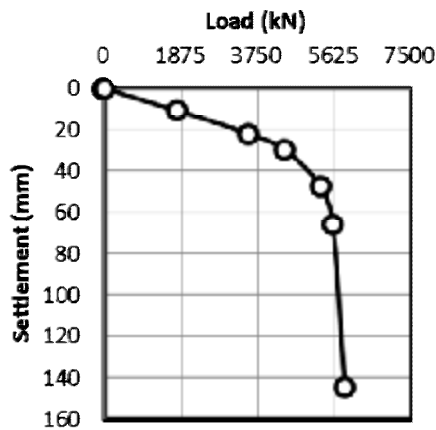


Figure (11) Load-Settlement relation of pile with D= 120 cm and L= 1800 cm.

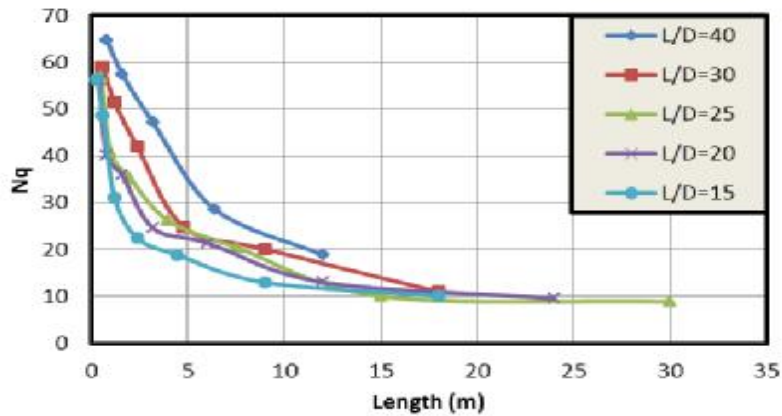


Figure (12) Bearing capacity factor N_q vs. length for all piles embedded in dense sand.

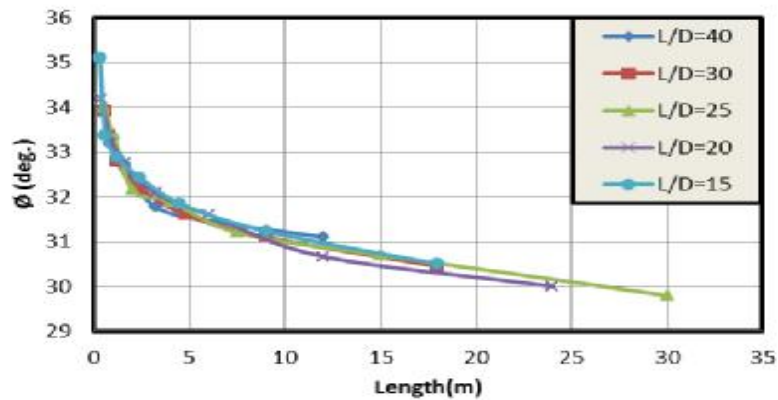


Figure (13) Mobilized angle of internal friction in the element below pile tip vs. length for piles embedded in dense sand measured at a settlement of (10% D).

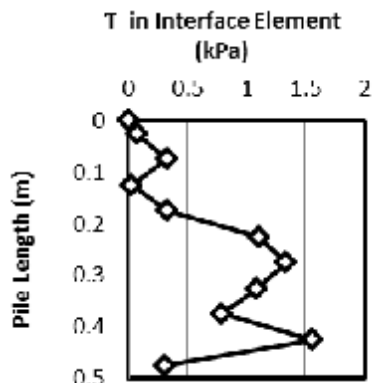


Figure (14) Shear stresses at soil-pile interface for pile with $D=2$ cm, $L=0.5$ m.

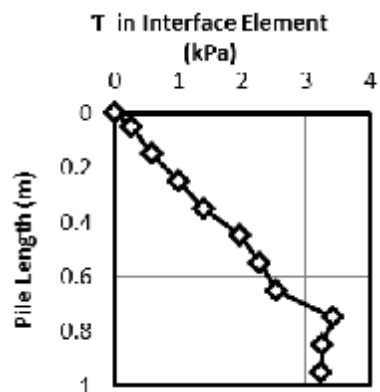


Figure (15) Shear stresses at soil-pile interface for pile with $D=4$ cm, $L=1$ m.

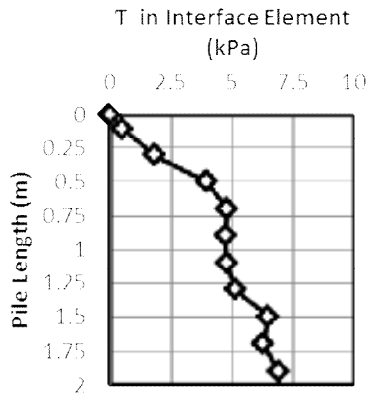


Figure (16) Shear stresses at soil-pile interface for pile with D= 8 cm, L=2m.

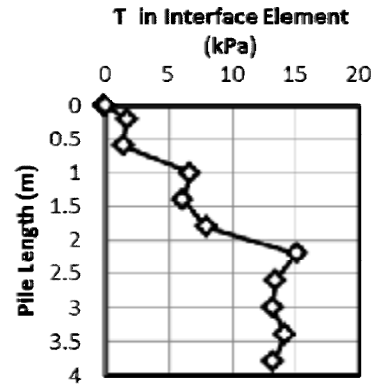


Figure (17) Shear stresses at soil-pile interface for pile with D= 16 cm, L=4m.

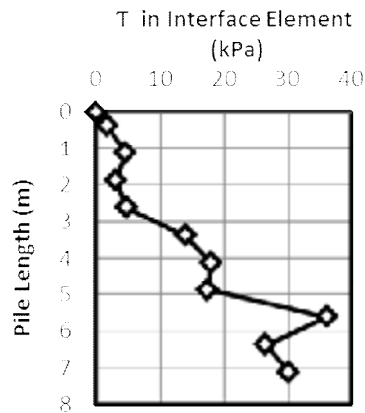


Figure (18) Shear stresses at soil-pile interface for pile with D=30 cm, L=7.5 m.

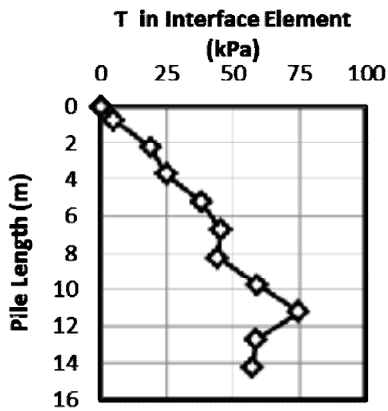


Figure (19) Shear stresses at soil-pile interface for pile with D= 60 cm, L= 15m.

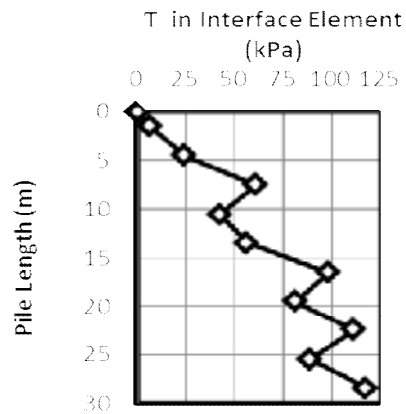


Figure (20) Shear stresses at soil-pile interface for pile with D= 120 cm, L= 30 m.

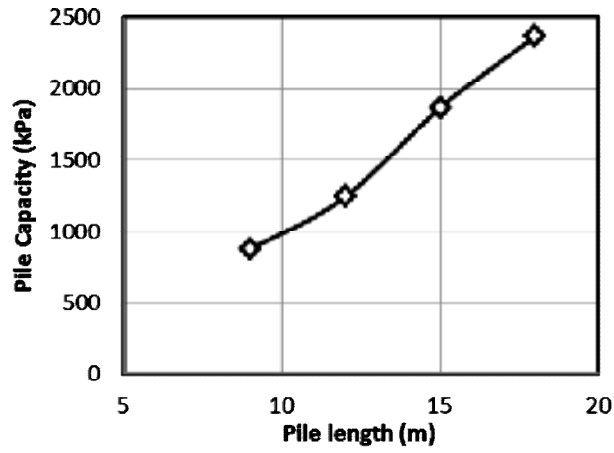


Figure (21) Pile length versus pile capacity relation of piles with diameter 60 cm.